



Optical Absorption and Scattering Properties of The Active Layer Of Perovskite Solar Cells Incorporated Silver Nanoparticles

PANUWAT CHAIYACHATE¹ and THANANCHAI DASRI^{2,3*}

¹School of Science and Mathematics, Faculty of Industrial and Technology, Rajamangala University of Technology Isan Sakon Nakhon Campus, Sakon Nakhon, 47160, Thailand.

²Faculty of Applied Science and Engineering, Khon Kaen University, Khon Kaen, 40002, Thailand.

³The Natural Resources, Energy and Environmental Research Sector (NEE), Khon Kaen University, Khon Kaen, 40002, Thailand.

*Corresponding author E-mail: thananchai_dasri@hotmail.com

<http://dx.doi.org/10.13005/ojc/330228>

(Received: February 11, 2017; Accepted: April 04, 2017)

ABSTRACT

This article presents the optical properties of pure silver (Ag) nanoparticle embedded in perovskite layer of perovskite solar cells using the discrete dipole approximation method (DDA). The influences of the Ag nanosphere size, shapes, and direction of the polarization direction of incident light respect to the particle axis on the absorption and scattering efficiencies on the localized surface plasmon resonance (LSPR) were investigated. For the single Ag nanoparticle, the calculated absorption and scattering spectra with increasing Ag diameter from 10 to 40 nm, both absorption and scattering resonance peaks were found at the position of around 624 nm. However, the optical efficiencies increases further with increasing the particle size up to 40 nm. For the optical properties of the two Ag nanoparticles with fixed 20 nm diameter and varying inter-particles spacing, the aligning particles perpendicular to both the propagation and polarization direction of light the increasing of the inter-particles spacing produces the shorter wavelength shift of the position peaks. In contrast, aligning particles perpendicular to the propagation direction and parallel to the polarization direction of light they were slightly shifted to longer wavelength as the inter-particles spacing increase. Finally for single Ag nanowire with varying the length of nanowire from 36.88 to 104.40 nm, both the absorption and scattering efficiencies peaks position get longer wavelength linearly shifted when the particlesax is was aligned perpendicular to the propagation direction and parallel to the polarization direction of light. However, they shift to shorter wavelength when the particlesax is was aligned both perpendicular to the propagation direction and the linear polarized light.

Keywords: Plasmonic nanoparticles, Perovskite solar cell, Discrete dipole approximation

INTRODUCTION

The metal nanoparticles (NPs) such as gold (Au), silver (Ag) and copper (Cu) which possess a negative real and small positive imaginary dielectric constant in thin films or nanostructures are potential candidates in many applications such as sensors¹, organic light-emitting devices (OLEDs)² and organic solar cells³⁻⁶ due to their localized surface plasmon resonance (LSPR). LSPRs are collective oscillations of a conductor's surface electrons at the interface between the metal NPs which much smaller than incident light wavelength and a dielectric medium under excited electromagnetic field that tend to trap optical waves near their interface⁷. The operation of the plasmonic nanoparticles in the above applications is affected by the refractive index of the metal and the surrounding medium, the particle size and shape as well as the polarization direction of the incident light. In the case of the plasmonic nanoparticles shape, variety of shape such as nanospheres^{3,8-11}, nanocubes¹¹, nanoprisms¹², nanoflowers^{3,13} and nanorod^{3, 11, 14} have been reported as the source for generating LSPRs. Perovskite solar cells (PSCs), known as photovoltaic device, have been reported that they have rapidly attracted attention due to its advantageous features including less

expensive material for fabricating PSCs, and rapidly increasing device efficiency¹⁵⁻¹⁹. Recently, plasmonic nanoparticles have been reported that utilizing them in PSCs can improve the light absorption in perovskite material¹⁸⁻²². Various types of metal NPs like pure nanospheres²¹, core/shell nanospheres and nanorods^{18,19} were reported. This article will theoretically present the effect of LSPR introduced by Ag NPs on the optical properties in the active layer of PSCs by using discrete Dipole Approximation (DDA). It is one of the most frequently used numerical methods for computing optical properties such as scattering and absorption by arbitrary size, shape nano-geometry²². The study will be presented the influence of the geometry and concentration of Ag NPs on the optical properties. This study will contribute to better understanding the uses of metal NPs for enhancing PSCs performances.

EXPERIMENTAL

Computational details

The absorption and scattering efficiencies of the pure Ag NPs were simulated based on the DDA theory²². This theory, the object in arbitrary shape is replaced with an assembly of N point dipoles in which the polarizability and positions are specified as α_i and

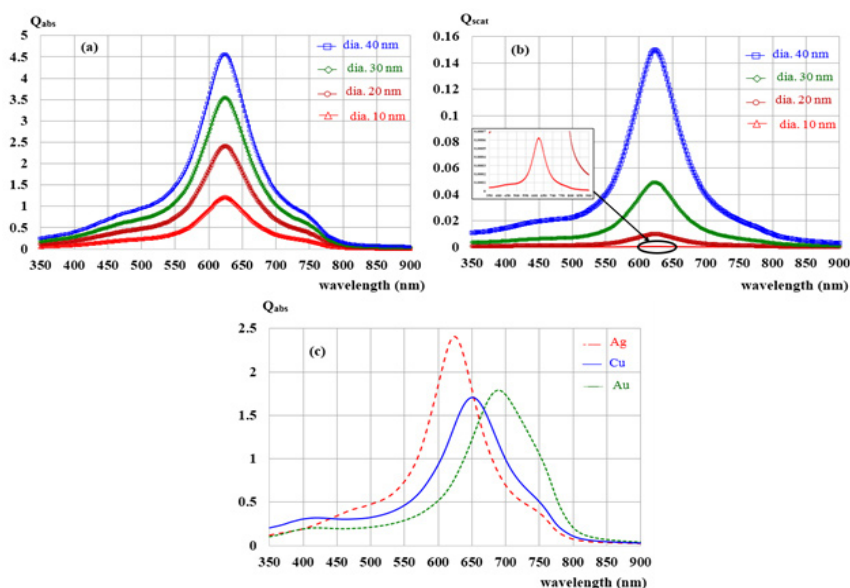


Fig. 1: (a) The absorption efficiency and (b) scattering efficiency for the Ag nanoparticle with varying their sizes. (c) Absorption efficiency for Ag, Au and Cu nanoparticles of a 10 nm radius. The insets in (a) shows the spectra in selected wavelength length.

r_p , respectively. The polarization induced \mathbf{P}_i in each particle in the presence of an applied field is then described by Eq.(1):

$$\bar{\mathbf{P}}_i = \alpha_i \bar{\mathbf{E}}_{\text{loc}}(\bar{\mathbf{r}}_i) \quad \dots(1)$$

where $\bar{\mathbf{E}}_{\text{loc}}$ is the sum of the incident field and the contribution from all other N-1 dipoles. When this polarization is obtained, the absorption, scattering and extinction cross sections of light can be calculated by Eqs. (2)- (4):

$$C_{\text{ext}} = \frac{4\pi k}{|E_0|^2} \sum_{i=1}^N \text{Im}(\bar{\mathbf{E}}_{\text{inc},i}^* \cdot \bar{\mathbf{P}}_i), \quad \dots(2)$$

$$C_{\text{abs}} = \frac{4\pi k}{|E_0|^2} \sum_{i=1}^N \left[\text{Im}[\bar{\mathbf{P}}_i \cdot (\alpha_i^{-1})^* \bar{\mathbf{P}}_i] - \frac{2}{3} k^3 |\bar{\mathbf{P}}_i|^2 \right], \quad \dots(3)$$

$$C_{\text{scat}} = C_{\text{ext}} - C_{\text{abs}}. \quad \dots(4)$$

Equations (2) and (3), ** symbol stands for the conjugate of a complex variable, k is the wave number and E_0 is the amplitude of incident electric field. And scattering, absorption and extinction efficiencies can be calculated by $Q_{\text{scat}} = C_{\text{scat}}/\pi R^2$, $Q_{\text{ext}} = C_{\text{ext}}/\pi R^2$ and $Q_{\text{abs}} = C_{\text{abs}}/\pi R^2$, respectively. R is radius of spherical nanoparticle. The dimensions of the morphologies Ag NPs were taken from Pathak *et al.*¹⁸. The refractive indices of Methylammonium lead triiodide ($\text{CH}_3\text{NH}_3\text{PbI}_3$) were taken from Löper *et al.*²³. The dielectric constants for metal NPS were obtained by using Lorentz-Drude model²⁴.

RESULTS AND DISCUSSIONS

The following results are the absorption and scattering efficiencies of Ag nanoparticles consisting of a single homogeneous spherical particle, two homogeneous spherical particles and nano wire at a fixed the surrounding medium refractive indices of $\text{CH}_3\text{NH}_3\text{PbI}_3$. At the first stage of this research,

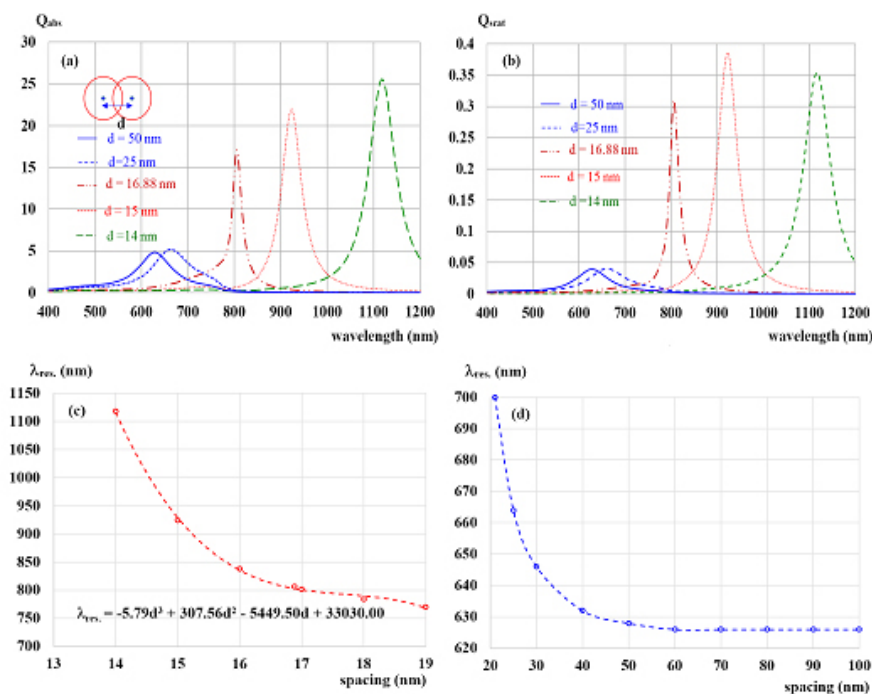


Fig. 2: Calculation of the spectral: (a) absorption and (b) scattering efficiencies as function of wavelength for two closely spaced Ag spherical particles, aligned perpendicular to the propagation direction and parallel to the linear polarized light. The spacing between two particles are indicated in the inset. (c) Shows effect of the overlapped and (d) non-overlapped distance between two Ag nanoparticles and the absorption peak position from (a). The diameters of two-Ag spherical particles were fixed of 20 nm.

the calculated absorption and scattering efficiencies of the single Ag nanoparticle with varying particle radius were presented, shown in Figs. 1a and 1b, respectively. It was observed that with increasing Ag diameter from 10 to 40 nm, absorption and scattering resonance peaks were found at the position of around 624 nm, but the peak intensity exhibits more as the

diameter increase. In Fig. 1c the optical property of Ag NPs was compared with the spectra obtained from Au and Cu nanoparticle. Clearly that the intensity of efficiency obtained from Ag nanoparticle is higher than Ag and Cu nanoparticle. For Au and Cu nanoparticle, the absorption resonance peaks are found at wavelength of ~690, and ~650 nm,

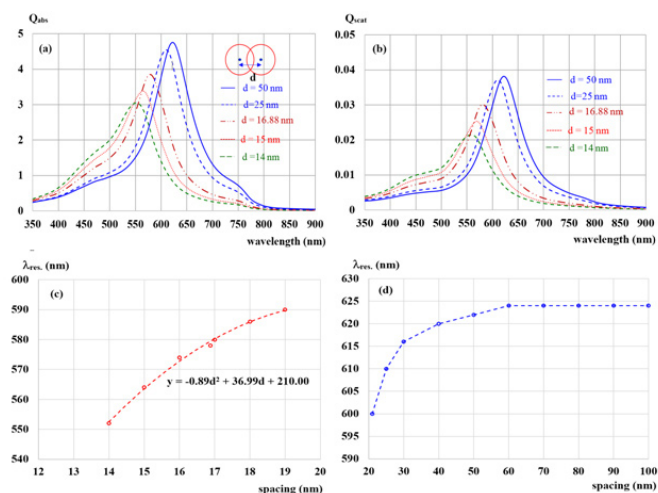


Fig. 3: Simulated of the spectral: (a) absorption and (b) scattering efficiencies as function of wavelength for two closely spaced Ag spherical particles, aligned perpendicular to both propagation direction and the linear polarized light. The spacing between two particles are indicated in the inset. (c) Shows effect of the overlapped and (d) non- overlapped distance between two Ag nanoparticles and the absorption peak position from (a). The diameters of two-Ag spherical particles were fixed of 20 nm.

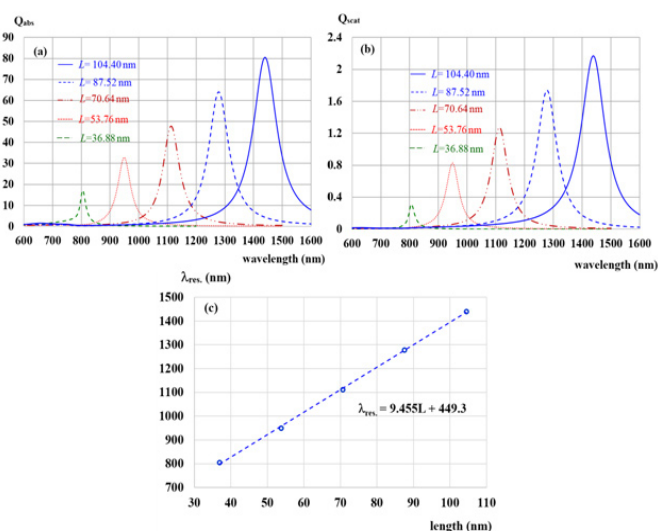


Fig. 4: Simulated (a) absorption and (b) scattering spectra of fixed 20 nm width Ag Nanowires aligned perpendicular to the propagation direction and parallel to the linear polarized light for the different length nanowires, L . (c) Absorption peak position from (a) as a function of nanowire length (red circles) plotted with a fitted linear curve (blue curves).

respectively, as seen in Fig. 1c. The presented results are indicated that the LSPRs are observed for Ag, Au and Cu nanoparticles in the visible wavelength region. This enhancement of in both absorption and scattering are due to the large electromagnetic field enhancement near the surface of these metal nanoparticles. In addition, the increase in the density of electrons as the size of metal nanoparticles increase results in the optical enhancement. The density of electrons in the metal nanoparticles influences the LSPRs of metal nanoparticles, which provides the enhancement of the absorption and scattering processes²⁵. Figures 2 and 3 are the optical absorption and scattering efficiencies for the two basic two-particle geometries. In these calculation, the diameters of two spherical homogeneous particle were fixed at 20 nm. In addition, the inter-particles distances were varied ranging from 14 to 100 nm. Fig. 2 presents the absorption efficiencies (Fig. 2a) and scattering efficiencies (Fig. 2b) for two particles aligned perpendicular to the propagation direction and parallel to the linear polarized light. The results show as the dipole spacing increases more, the optical efficiencies peak position shift to longer wavelength. For example it shifts approximately ~1,118 nm for dipoles with a 14 nm spacing. By fitting the relation between optical efficiencies peak position and the dipole spacing, it found that the absorption peak shifts to longer wavelength nonlinearly with the increasing of the dipole spacing

(14-19 nm which overlaps each other) shown in Fig. 2c. The numerical calculation result was fitted by the polynomial function $\lambda_{res}[\text{nm}] = -5.79d^3 + 307.56d^2 - 5449.50d + 33030$, where λ_{res} and d being the peak position and dipole spacing, respectively. In contrast, non-overlapping of two Ag nanospheres was found that the absorption peak shifts to longer wavelength nonlinearly with exponential-like decrease function as seen in Fig. 2d. However, as the inter-particles spacing were varied from 60 to 100 nm, non-shifting of the absorption peak was found. Whereas, Fig. 3 are the theoretical results for two particles aligned perpendicular to both propagation direction and the linear polarized light. In contrast with another geometry, shorter wavelength-shifting was observed in these calculations down to ~552 nm at a 14 nm spacing. Fig. 3c shows that the absorption peak shifts to shorter wavelength nonlinearly with the increasing of the inter-particles spacing of Ag nanoparticles. The best fitted in the case of overlapping of two Ag nanospheres was found as the polynomial function $\lambda_{res}[\text{nm}] = -0.895d^2 + 36.99d + 210$. In contrast, non-overlapping of two Ag nanospheres was found that the absorption peak shifts to longer wavelength nonlinearly with exponential-like decrease function as seen in Fig. 3d. However, as the inter-particles spacing were in the range of 60-100 nm, non-shifting of the absorption peak was found similar with the other case. Further more, Figs. 4 and 5 present the simulated absorption and scattering efficiencies

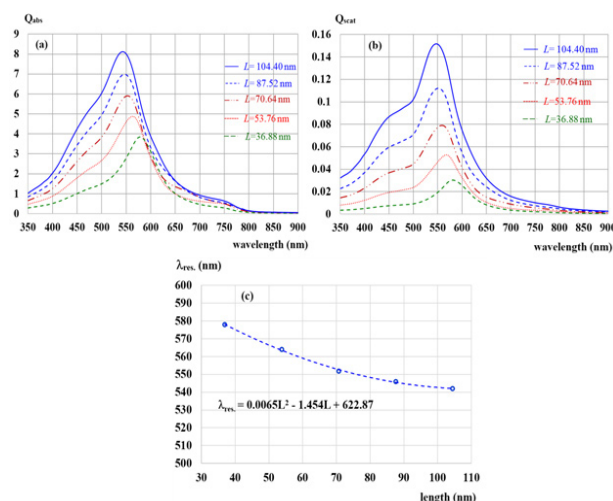


Fig. 5: Simulated (a) absorption and (b) scattering spectra of fixed 20 nm width Ag Nanowires aligned perpendicular to both the propagation direction and the linear polarized light for the different length nanowires, L . (c) Absorption peak position from (a) as a function of nanowire length (red circles) plotted with a fitted linear curve (blue curves).

spectra of fixed 20 nm width Ag nanowires as a function of wavelength with different nanowire length ($L = 36.88, 53.76, 70.64, 87.52$ and 104.40 nm). The nanowire axis in Fig. 4 was aligned perpendicular to propagation direction and parallel to the linear polarized light and bigger, whereas in Fig. 5, it was orthogonal to both propagation direction and the linear polarized light. The results were found that the longer wavelength-shifted of the surface plasmon both absorption and scattering peaks with increasing nanowire length for the first case as seen in Figs. 4a and 4b, however distinct shorter wavelength-shifted is observed for the other case shown in Figs. 5a and 4b. The maximum shifted of optical spectra in Fig. 4 was found at the wavelength of ~ 1440 nm for the 104.4 nm nanowire length. The spectral peak position as a function of nanowire length is shown in Fig. 4c. The best fitted was found as the linear function $\lambda_{res} [\text{nm}] = 9.455L + 449.3$, where L is the peak position and nanowire length. Whereas, the maximum shifted of optical spectra in Fig. 5 was observed at the wavelength of ~ 578 nm for the smaller nanowire length ($L = 36.88$ nm). The spectral peak position as a function of nanowire length in this case was found as the polynomial function $\lambda_{res} [\text{nm}] = 0.0065L^2 - 1.454L + 622.87$. The shifted resonance peak position can be qualitatively discussed²⁶ that due to the object in arbitrary shape in DDA model is replaced with an assembly of N point dipoles. Therefore, the aligning particles axis parallel to the polarized light direction the plasma electron distributions of all particles is therefore perturbed with weakening of the repulsive forces of the field. This effect leads to a correspondingly lower

resonance frequency or longer wavelength as seen in the simulated results Figs. 2 and 4. In contrast, when the excited electric field incidents normal to the longer particles axis the charge distributions of each particle acts cooperatively to enhance the repulsive action in all particles, thus decreasing the resonance wavelength as seen in Figs. 3 and 5. Moreover, the obtained results found that it is possible to shift the LSPRs frequency into the near-infrared region (NIR) of the spectrum by increase the inter-particles distance as seen in Fig. 2 and nanowire length of the silver nanoparticles as seen in Fig. 4.

CONCLUSION

In summary, the absorption and scattering efficiencies of the Ag nanoparticle with varying their size, shape and direction polarization of the linear polarized light were studied using the DDA method. The results found that the incorporating of Ag nanoparticle in the active layer of PSC shows strongly LSPR induced. Moreover, the results revealed that the resonance peak of LSPR can be tuned over wavelength from the visible to the near-infrared region of the spectrum. Thus, the basic results of this study might be used for basic fabricating the more performance PSCs.

ACKNOWLEDGMENTS

The authors are grateful to the Faculty of Applied Science and Engineering, Nong Khai Campus, Khon Kaen University for all facilities supported.

REFERENCES

- Huang, M.; Zhang, Y.; Du, C.; Peng, S.; Shi, D. *Plasmonics* **2016**, *11*, 1197-1200
- Tang, M.; Zhu, W.; Sun, L.; Yu, J.; Qian, B.; Xiao, T. *Synth. Met.* **2015**, *199*, 69-73
- Kozanoglu, D.; Apaydin, D. H.; Cirpan, A.; Esenturk, E. N. *Org. Electron.* **2013**, *14*, 1720-1727.
- Liu, F.; Xie, W.; Xu, Q.; Liu, Y.; Cui, K.; Feng, X.; Zhang, W.; Huang, Y. *IEEE Photonics J.* **2013**, *5*, 8400509
- Cheng, C.-E.; Pei, Z.; Hsu, C.-C.; Chang, C.-S.; Chien, F. S.-S. *Sol. Energy Mater. Sol. Cells*, **2014**, *121*, 80-84
- Notarianni, M.; Vernon, K.; Chou, A.; Aljada, M.; Liu, J.; Motta, N. *Sol. Energy*, **2014**, *106*, 23-37
- Barnes, W.L.; Dereux, A.; Ebbesen, T.W. *Nature*, **2003**, *424*, 824-830
- Dasri, T.; Sompech, S. *Integrated Ferroelectrics*, **2015**, *165*, 176-184
- Sompech, S.; Thaomola, S.; Dasri, T. *Oriental J. Chem.* **2016**, *32*, 85-91
- Ranjgar, A.; Zolanvari, A.; Sadeghi, H. *Plasmonics* **2016**, *11*, 277-284

11. Dasri, T. *Integrated Ferroelectrics***2016**, *175*, 176–185
12. Viarbitskaya, S.; Cucho, A.; Teulle, A.; Sharma, J.; Girard, C.; Arbouet, A.; Erik Dujardin, E. *ACS Photonics***2015**, *2*, 744–751
13. Garjan, A. S.; Savaloni, H. *EPJ B***2013**, *86*, 257-270
14. Cao, J.; Sun, T.; Grattan, K. T. V. *Sens. Actuators, B***2014**, *195*, 332–351
15. Park, N. G. *Mater. Today***2015**, *18*, 65–72
16. Green, M. A.; Ho-Baillie, A.; Snaith, H. J. *Nat. Photonics* **2014**, *8*, 506–514
17. Yang, Z.; Zhang, W. H. *Chin. J. Catalysis*, **2014**, *35*, 983–988
18. Pathak, N. K.; Chander, N.; Komarala V K, Sharma, R. P. *Plasmonics*, **2016**, 1-8
19. Cui, J.; Chen, C.; Han, J.; Cao, K.; Zhang, W.; Shen, Y.; Wang, M. *Adv. Sci.***2016**, *3*, 1500312
20. Yue, L.; Yan, B.; Attridge, M.; Wang, Z. *Sol. Energ.* **2016**, *124*, 143-152
21. Carretero-Palacios, S.; Jiménez-Solano A.; Míguez, A. *ACS Energy Letters*, **2016**, *1*, 323-331
22. Purcell, E.M.; Pennypacker, C. R. *Astrophys J.***1973**, *186*, 705-714
23. Löper, P.; Stuckelberger, M.; Niesen, B.; Werner, J.; Filipic, M.; Moon, S. –J.; Yum, J. –H.; Topic, M.; Wolf, S. D.; Ballif, C. J. *Phys. Chem. Lett.***2015**, *6*, 66–71
24. Rakia, A. D.; Djurišić, A. B.; Elazar, J. M.; Majewski, M. L. *Appl. Opt.***1998**, *37*, 5271-5283
25. Pradhan, A. K.; Konda, R. B.; Mustafa, H.; Mundle, R.; Bamiduro, O.; Roy, U. N.; Cui, Y.; Burger, A. *Opt. Express*, **2008**, *16*, 6202–6208
26. Rechberger, W.; Hohenau, A.; Leitner, A.; Krenn, J. R.; Lamprecht, B.; Aussenegg, F. *Opt. Commun.***2003**, *220*, 137–141